

Communication

Silver Nanoplate Composites as Nonlinear Saturable Absorbers for a Q-Switched Laser

Wenhao Lyu ^{1,†}, Yuan Cheng ^{1,†}, Jiayi An ¹, Marcello Condorelli ², Mario Pulvirenti ², Giuseppe Compagnini ², Xiaogang Wang ³, Bo Fu ^{1,3,*} and Vittorio Scardaci ^{2,*}¹ School of Instrumentation and Optoelectronic Engineering, Beihang University, Beijing 100191, China² Dipartimento di Scienze Chimiche, Università Degli Studi di Catania, 95125 Catania, Italy³ Key Laboratory of Big Data-Based Precision Medicine Ministry of Industry and Information Technology, School of Engineering Medicine, Beihang University, Beijing 100191, China

* Correspondence: fubo10@buaa.edu.cn (B.F.); vittorio.scardaci@unict.it (V.S.)

† These authors contributed equally to this work.

Abstract: Metal nanomaterials have promising applications in ultrafast photonics due to their broad-band operation, large third-order nonlinear susceptibility, and ultrafast recovery time. We realized a Q-switched pulsed erbium-doped fiber laser based on a silver nanoplate polyvinyl alcohol film as a saturable absorber. This film, with a modulation depth of 15.7%, was integrated into a fiber laser by means of a sandwich structure. We obtained Q-switched pulses in the 1.5- μm band, which plays an important role in telecommunications and atmospheric detection. Stable Q-switched pulses were obtained at the pump power of 135 mW, with a single pulse energy of 33.8 nJ, a pulse width of 2.3 μs , a repetition rate of 62.4 kHz, and a signal-to-noise ratio of about 45 dB. When increasing the pump power up to a maximum value of 246 mW, the maximum single pulse energy of 57.8 nJ was achieved. This study first demonstrates the potential of silver nanoplates as saturable absorbers in generating stable laser pulses with high energy.

Keywords: Q-switched laser; erbium-doped fiber laser; silver nanoplates; saturable absorber

Citation: Lyu, W.; Cheng, Y.; An, J.; Condorelli, M.; Pulvirenti, M.; Compagnini, G.; Wang, X.; Fu, B.; Scardaci, V. Silver Nanoplate Composites as Nonlinear Saturable Absorbers for a Q-Switched Laser. *Photonics* **2022**, *9*, 835. <https://doi.org/10.3390/photonics9110835>

Received: 17 October 2022

Accepted: 4 November 2022

Published: 7 November 2022

Publisher's Note: MDPI stays neutral with regard to jurisdictional claims in published maps and institutional affiliations.



Copyright: © 2022 by the authors. Licensee MDPI, Basel, Switzerland. This article is an open access article distributed under the terms and conditions of the Creative Commons Attribution (CC BY) license (<https://creativecommons.org/licenses/by/4.0/>).

1. Introduction

Pulsed lasers have attracted extensive research efforts in the field of laser ranging [1], optical fiber sensing [2], spectral analysis [3], and medical photonics [4]. With the capability to generate pulses with a narrow bandwidth and high energy, pulsed lasers have a vital practical value. Mode-locking and Q-switching are the two main techniques for obtaining laser pulses [5–8]. The former usually requires fixed phases of longitudinal modes in the laser cavity, resulting in pulses with a narrow bandwidth and a high repetition rate. The latter refers to adjusting the loss in a laser cavity and generating pulses with extremely high energy. There exist multiple methods to realize mode-locked and Q-switched lasers, such as nonlinear polarization rotation (NPR) [9], a nonlinear amplifying loop mirror (NALM) [10], a semiconductor-saturable absorber mirror (SESAM) [11], and saturable absorbers (SAs) based on nanomaterials [12–21]. Owing to the outstanding nonlinear optical properties, these methods have good performance in the realization of pulsed lasers. However, NPR and NALM have bulky structures, which require complex adjustments. As the classical real SA, SESAM is limited by high fabrication cost and narrow operating bandwidth. Nanomaterials assist the generation of pulsed lasers due to the properties of saturable absorption, which possess the advantages of low cost, simple fabrication, and convenient integration. In recent years, nanomaterials have been widely utilized in pulsed fiber lasers as SAs owing to their preeminent optical properties. The common nanomaterials employed as SAs include carbon nanotubes [22], graphene [23–25], black phosphorus [26,27], topological insulators [28,29], transition metal dichalcogenides [30,31], and MXenes [32,33]. In addition to these materials, metal nanomaterials have also attracted

extensive attention due to their excellent nonlinear optical properties [34]. Very recently, Li et al. used reduced graphene oxide-tricobalt tetroxide composites to obtain stable mode-locked pulses, showing a feasible method to prepare SA materials [35]. In addition, alloy films and metal oxides can also be utilized as nonlinear SAs due to their advantages [36,37].

Metal nanomaterials have tunable surface plasmon resonance (SPR), remarkable nonlinear optical properties, as well as ultrafast recovery time, which make them promising candidates as SA materials [38–41]. In general, the SPR of metal nanomaterials varies with their microscopic morphology, size, and environmental factors [42,43], which also indicates that metal nanomaterials have a bright prospect in the field of photonics. Gold nanomaterials, as the most common metal nanomaterials, include various forms such as nanoparticles, nanorods, nanowires, and nanoplates. These gold nanomaterials could be used as SAs in fiber lasers to achieve stable mode-locked or Q-switched pulses at the main wavelengths of 1, 1.5, and 2 μm [44–47]. Silver nanomaterials, showing superior optical properties comparable to gold nanomaterials, such as possessing large third-order nonlinear optical properties and broadband operation [48–51], have also been investigated for laser pulse generation [52–55]. Erbium-doped fiber lasers (EDFLs) utilizing silver nanoparticle SAs have been extensively studied, while employing silver nanoplates (SNPTs) as SAs to realize pulsed lasers at 1.5 μm has not been explored so far to our knowledge. Compared with carbon nanotubes and 2D nanomaterials, SNPTs have interesting SPR properties. The SPR-related optical properties make SNPTs a promising SA with broadband operation and large third-order nonlinear polarizability [56]. In addition, using polyvinyl alcohol (PVA) to form a composite film is a convenient and efficient integration method. In 2012, Sackuvich et al. implemented a middle-infrared (mid-IR) laser by using a silver-based composite material [57]. In 2017, Cesca et al. experimentally investigated the nonlinear absorption property of Ag nanoprism arrays, indicating the excellent nonlinear optical responses of Ag nanomaterials [58]. In 2019, Rosdin et al. achieved stable mode-locked pulses in EDFL using a silver nanoparticle film on PVA as the SA [53]. However, the silver nanoparticle film was synthesized by a thermal evaporation process in a vacuum environment with a complex preparation process and poor control of the film morphology. The SNPTs used in our paper were fabricated by wet chemistry processing, which is more convenient and allows better control of the morphology and optical properties of silver nanomaterials [43].

In this paper, SNPT-based SAs were used to realize Q-switched EDFL. We employed the seed-mediated growth process for the synthesis of SNPTs by controlling the volume of seed solution to obtain appropriate SNPTs. To integrate those nanoplates into the ring laser cavity, we compounded our nanoplates with PVA, which were formed into a thin film with high light transmittance. Then, the SNPT-PVA film was integrated into the laser cavity with a sandwich structure. Furthermore, we measured the saturable absorption capability of the SNPT-PVA film and obtained a modulation depth of about 15.7%. The laser structure featured a 0.5 m erbium-doped gain fiber and incorporated an SNPT-PVA film for a total cavity length of around 7 m. The stable Q-switched laser pulses were obtained by increasing the pump power to 135 mW, possessing a central wavelength of 1563.3 nm and a pulse width of 2.3 μs , while the output single pulse energy was around 33.2 nJ. Upon increasing the pump power to the maximum value of 246 mW, the maximum single pulse energy of 57.8 nJ was achieved. To the best of our knowledge, EDFLs utilizing SNPTs as nonlinear SAs for Q-switched lasers has not been explored. In this work, the results indicate that SNPTs can be promising candidates for obtaining high-energy Q-switched pulses.

2. Fabrication and Characterization

Triangular SNPTs were synthesized by the well-known seed-mediated growth method [59]. In an aqueous environment containing citrate, silver nitrate (AgNO_3 , 99% purity from Merck, Kenilworth, NJ, USA) was reduced by sodium boron hydrate to form spherical silver nanoparticles (SNPs), or seeds. Such SNPs were converted to triangular SNPTs by using a set volume of the seed solution to which further citrate, hydrazine, and AgNO_3

were added. The volume of the seed solution could affect the size of the materials, which would further influence the SPR of the SNPTs. Utilizing a smaller amount of solution would produce SNPTs with larger sizes, displaying SPR in the near-infrared band [59]. To achieve SPR in the near IR, especially close to 1550 nm, very large nanoplates have to be synthesized [49]. Herein, a volume of $\sim 5 \mu\text{L}$ of seeds solution was used. The citrate was used for both stabilizing the SNPTs in solution as a ligand and directing the seed growth by binding preferentially to the (111) facets of Ag [60]. However, as citrate is transparent in the whole range, this would not affect the property of the SA.

As shown in Figure 1a, the scanning electron microscopy (SEM) image of the SNPTs taken from the starting solution reveals that most of the SNPs have grown into a mixture mainly containing triangular nanoplates. Figure 1b shows the atomic force microscope (AFM) image of the SNPTs. Compared with the SEM image, the micromorphology of our SNPTs is clearer in the AFM image. It can be observed that the grown SNPTs are about 200 nm in size. Besides, the yield of nanoplates is a mixture of shapes, containing mainly triangular nanoplates.

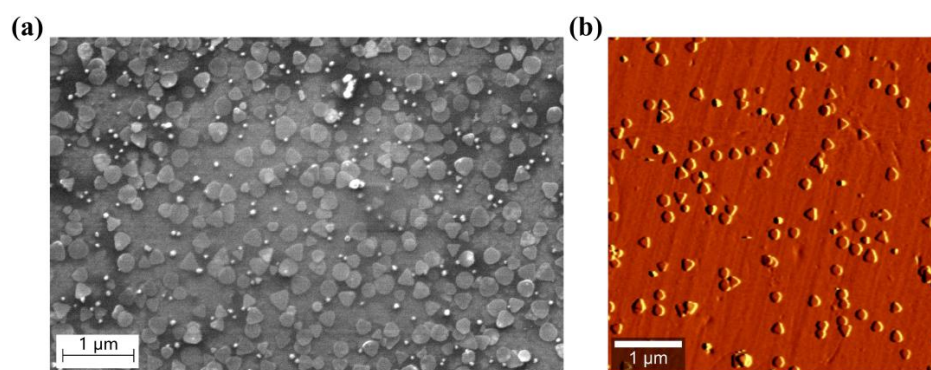


Figure 1. Microscopic images of SNPTs. (a) SEM image. (b) AFM image.

In order to obtain the composite film, an aliquot of the SNPT solution was mixed under stirring with 2 mL PVA aqueous solution (50 g/L) and let dry under ambient conditions in a plastic Petri dish. The PVA was applied to form a relatively closed space, thus making the materials relatively robust. Breaking the petri dish left a freestanding SNPT-PVA film. Then, we measured the absorption spectrum shown in Figure 2 by using an ultraviolet and visible spectrophotometer (Agilent Cary 60, Santa Clara, CA, USA). It can be seen that there is a small absorption peak at about 450 nm, likely arising from residual seeds, and a broad absorption band from 800 nm to 1600 nm, thus comprising our target wavelength at 1.5 μm . The marked areas indicate the range of typical working wavelength for the erbium-doped fiber laser (yellow band in Figure 2).

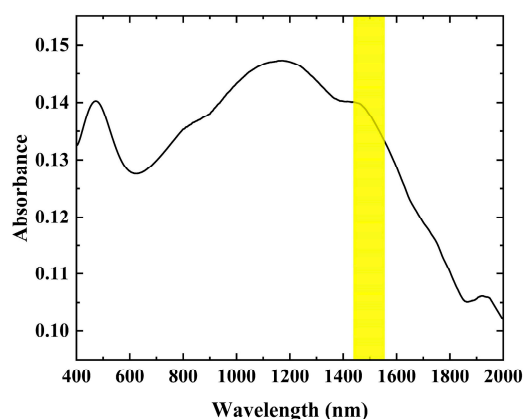


Figure 2. Absorption spectrum of SNPT-PVA composite. The yellow band indicates the typical working wavelength for an EDFL.

With the purpose of further analyzing the nonlinear absorption characteristics of the SNPT-PVA film in the 1.5- μm band, we used the nonlinear transmission measurement setup shown in Figure 3. This twin detector method could measure the modulation depth of the SNPT-PVA composite and obtain the nonlinear saturable absorption curve shown in Figure 4. The laser source could output a stable mode-locked laser at 1.5 μm . A variable optical attenuator (VOA) was used to adjust the pulse energy. After the output coupler (OC), the laser was split into two beams, passing through two paths with and without an SNPT-based SA. The output power was finally measured by a power meter. Two sets of data were obtained, representing the input and output power of the pulses passing through the SNPT-based SA. By integrating the two sets of data, the relationship curve between the transmittance and input power was acquired. In addition, the modulation depth was calculated from the difference between the maximum and minimum transmittance of the curve. We can observe from the curve in Figure 4 that the SNPT-PVA film has a saturable absorption characteristic with a modulation depth of around 15.7%, which confirms the potential to become an SA.

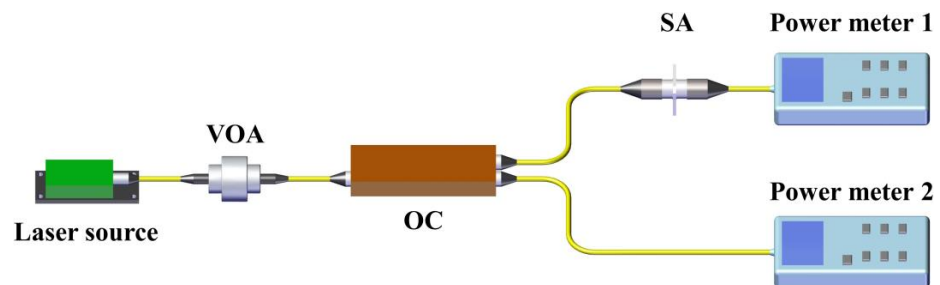


Figure 3. Setup of nonlinear transmission measurement. VOA: variable optical attenuator; OC: output coupler; SA: saturable absorber.

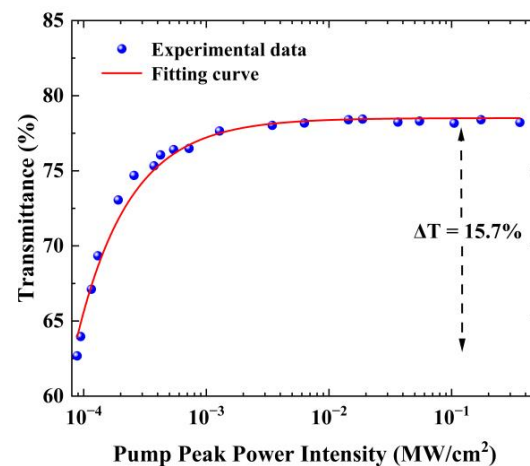


Figure 4. Nonlinear saturable absorption curve of the SNPT-based SA.

3. Schematic of the Passively Q-Switched Fiber Laser

The setup of the EDFL ring cavity is shown in Figure 5, in which the SNPT-PVA film was used as the SA. Moreover, a 0.5 m EDF was employed as the gain medium. A 980 nm laser diode (LD), used as the pump source, was injected into the laser cavity by a wavelength-division multiplexer (WDM). Other components included a polarization-insensitive isolator (PI-ISO) to assure unidirectional propagation, a polarization controller (PC) to adjust polarization expediently, an output coupler (OC) with 20% output, and single-mode fibers in the cavity. Since each device had a certain pigtail length, the total length of the cavity was ~ 7 m.

The output parameters were monitored through an optical spectrum analyzer (Yokogawa AQ6375B, Musashino, Japan), a digital storage oscilloscope (Siglent SDS6104 H10

Pro, Shenzhen, China), a spectrum analyzer (Agilent N9320B), and an optical power meter (EXFO FPM-602X, Quebec, QC, Canada).

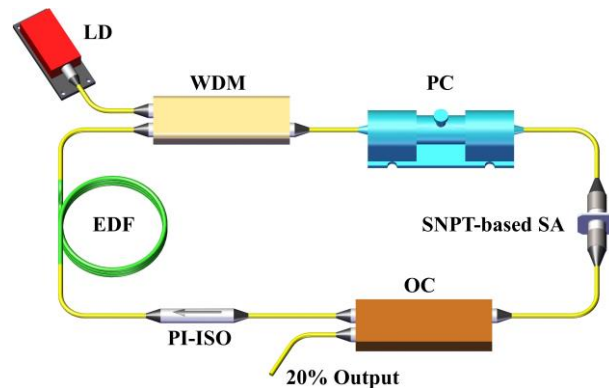


Figure 5. Setup of passively Q-switched fiber laser based on an SNPT-based SA. EDF: erbium-doped fiber; LD: laser diode; WDM: wavelength-division multiplexer; PC: polarization controller; SNPT: silver nanoplate; SA: saturable absorber; PI-ISO: polarization-insensitive isolator; OC: output coupler.

4. Results and Discussion

Originally, the continuous wave operation was first obtained at the pump power of 55 mW. The Q-switched pulses were obtained when the pump power reached 135 mW. Figure 6a shows the optical spectrum at the central wavelength of 1563.3 nm with a full width at half maximum of 0.3 nm. The Q-switched pulse train with a time interval of 16 μs is shown in Figure 6b, in line with the repetition rate of 62.4 kHz (Figure 6d). As shown in Figure 6c, the pulse duration of the Q-switched pulse is around 2.3 μs with a pulse energy of 33.8 nJ. The 45 dB signal-to-noise ratio (SNR) of the radio-frequency (RF) spectrum in Figure 6d indicates the stable operation of the laser. Figure 7a presents the output power as a function of the pump power, in which the maximum output power is 2.9 mW at the pump power of 246 mW. Meanwhile, the pulse energy as a function of pump power is shown in Figure 7b, where the pulse energy of the output pulses increases from 44.7 to 57.8 nJ. The error bars are presented in Figure 7, indicating that the Q-switched laser is relatively stable.

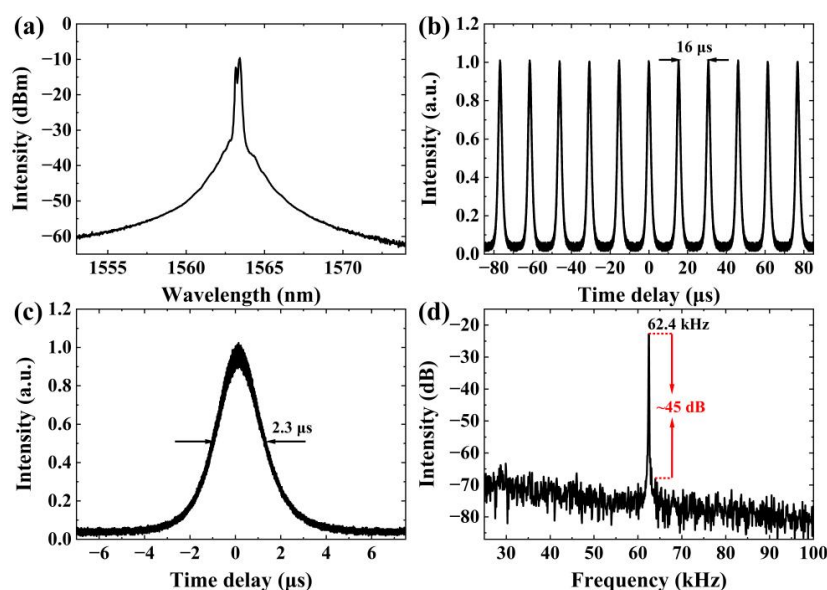


Figure 6. Experimental results of EDFL for a pump power of 135 mW. (a) Optical spectrum. (b) Q-switched pulse train. (c) Single pulse profile. (d) RF spectrum.

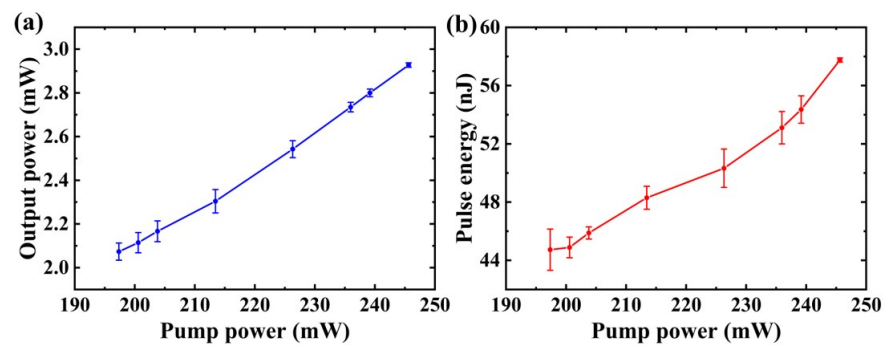


Figure 7. Q-switched laser features for different pump powers. (a) Average output power as a function of pump power. (b) Measured pulse energy as a function of pump power.

Ultimately, we compared the output performances of Q-switched EDFL using diverse metal-based SAs (including our work), as shown in Table 1. From the comparison table, the polymer film is still the mainstream method, in which PVA is widely used with high light transmittance. It should be noted that our Q-switched EDFL based on SNPTs obtained the highest output power and single pulse energy. In addition, the SNR of the Q-switched pulses we obtained is also comparable to other works. It can be concluded that SNPT is a potential SA to realize pulsed lasers with high energy and output power for a variety of applications.

Table 1. Comparison of Q-switched EDFL enabled by different metal-based SAs.

Metal-Based SA	Integration	SNR (dB)	Output Power (mW)	Pulse Energy (nJ)	Ref.
Fe ₃ O ₄	Deposition	-	0.794	23.76	[61]
NiO	Chitosan	43.3	-	15.3	[62]
ZnO	Polymer film	42	2.77	46	[63]
ITO	Deposition	-	1.72	21.16	[64]
TiO ₂	PVA	37	0.826	5.81	[65]
Au	PVA	-	1.4	44.29	[66]
Cu	PVA	50.9	1.86	18.38	[67]
Ag	PVA	45	2.9	57.8	This work

Fe₃O₄: ferroferric oxide; Ni: nickel; Zn: zinc; I: indium; T: tin; Ti: titanium; Au: gold; Cu: copper; Ag: silver; PVA: polyvinyl alcohol; SA: saturable absorber; SNR: signal-to-noise ratio.

5. Conclusions

We obtained a Q-switched EDFL based on an SNPT-PVA film, with an intracavity modulation ability at 1.5 μm by controlling the size of the SNPTs through the seed-mediated growth process. When the pump power reached 135 mW, stable Q-switched pulses were obtained at 1563.3 nm, with a repetition rate of 62.4 kHz and an SNR of about 45 dB. At the maximum pump power of 246 mW, we achieved the maximum pulse energy high up to 57.8 nJ. The experimental results show that SNPT-based SAs, prepared by seed-mediated growth, can generate Q-switched pulses with high energy in the EDFL, which is worthy of further exploration for multiple applications, such as telecommunication, biomedical photonics, and atmospheric detection.

Author Contributions: Conceptualization, B.F. and V.S.; methodology, B.F.; validation, G.C., X.W. and V.S.; formal analysis, W.L. and Y.C.; investigation, W.L.; resources, M.C. and M.P.; data curation, Y.C., M.C. and M.P.; writing—original draft preparation, W.L.; writing—review and editing, Y.C., J.A. and V.S.; supervision, G.C., X.W. and B.F. All authors have read and agreed to the published version of the manuscript.

Funding: This research was funded by the Beijing Natural Science Foundation (4202044), the National Natural Science Foundation of China (62071016, 62111530239, and 92049201), and the Fundamental Research Funds for the Central Universities (501LKQB2022145005).

Institutional Review Board Statement: Not applicable.

Informed Consent Statement: Not applicable.

Data Availability Statement: Not applicable.

Conflicts of Interest: The authors declare no conflict of interest.

References

1. Riemensberger, J.; Lukashchuk, A.; Karpov, M.; Weng, W.; Lucas, E.; Liu, J.; Kippenberg, T.J. Massively parallel coherent laser ranging using a soliton microcomb. *Nature* **2020**, *581*, 164–170. [[CrossRef](#)] [[PubMed](#)]
2. Di Teodoro, F.; Belden, P.; Ionov, P.; Werner, N.; Fathi, G. Development of pulsed fiber lasers for long-range remote sensing. *Opt. Eng.* **2014**, *53*, 036105. [[CrossRef](#)]
3. Sorokina, E.; Sorokina, I.T.; Mandon, J.; Guelachvili, G.; Picqué, N. Sensitive multiplex spectroscopy in the molecular fingerprint 2.4 μm region with a Cr^{2+} : ZnSe femtosecond laser. *Opt. Express* **2007**, *15*, 16540–16545. [[CrossRef](#)] [[PubMed](#)]
4. Allen, T.J.; Beard, P.C. Pulsed near-infrared laser diode excitation system for biomedical photoacoustic imaging. *Opt. Lett.* **2006**, *31*, 3462–3464. [[CrossRef](#)] [[PubMed](#)]
5. Hargrove, L.E.; Fork, R.L.; Pollack, M.A. Locking of He–Ne laser modes induced by synchronous intracavity modulation. *Appl. Phys. Lett.* **1964**, *5*, 4–5. [[CrossRef](#)]
6. Mocker, H.W.; Collins, R.J. Mode competition and self-locking effects in a Q-switched ruby laser. *Appl. Phys. Lett.* **1965**, *7*, 270–273. [[CrossRef](#)]
7. Karlitschek, P.; Hillrichs, G. Active and passive Q-switching of a diode pumped Nd:KGW-laser. *Appl. Phys. B* **1996**, *64*, 21–24. [[CrossRef](#)]
8. Sorokina, I.T.; Sorokin, E.; Di Lieto, A.; Tonelli, M.; Page, R.H.; Schaffers, K.I. Active and passive mode-locking of the Cr^{2+} : ZnSe laser. In Proceedings of the Advanced Solid State Lasers, Seattle, WA, USA, 28–31 January 2001.
9. Matsas, V.J.; Newson, T.P.; Richardson, D.J.; Payne, D.N. Selfstarting passively mode-locked fibre ring soliton laser exploiting nonlinear polarisation rotation. *Electron. Lett.* **1992**, *28*, 1391–1393. [[CrossRef](#)]
10. Aguergaray, C.; Broderick, N.G.R.; Erkintalo, M.; Chen, J.S.Y.; Kruglov, V. Mode-locked femtosecond all-normal all-PM Yb-doped fiber laser using a nonlinear amplifying loop mirror. *Opt. Express* **2012**, *20*, 10545–10551. [[CrossRef](#)]
11. Barnett, B.C.; Rahman, L.; Islam, M.N.; Chen, Y.C.; Bhattacharya, P.; Riha, W.; Reddy, K.V.; Howe, A.T.; Stair, K.A.; Iwamura, H.; et al. High-power erbium-doped fiber laser mode locked by a semiconductor saturable absorber. *Opt. Lett.* **1995**, *20*, 471–473. [[CrossRef](#)]
12. Bonaccorso, F.; Sun, Z. Solution processing of graphene, topological insulators and other 2d crystals for ultrafast photonics. *Opt. Mater. Express* **2013**, *4*, 63–78. [[CrossRef](#)]
13. Yao, B.C.; Rao, Y.J.; Wang, Z.N.; Wu, Y.; Zhou, J.H.; Wu, H.; Fan, M.Q.; Cao, X.L.; Zhang, W.L.; Chen, Y.F.; et al. Graphene based widely-tunable and singly-polarized pulse generation with random fiber lasers. *Sci. Rep.* **2015**, *5*, 18526. [[CrossRef](#)] [[PubMed](#)]
14. Liu, X.; Guo, Q.; Qiu, J. Emerging low-dimensional materials for nonlinear optics and ultrafast photonics. *Adv. Mater.* **2017**, *29*, 1605886. [[CrossRef](#)] [[PubMed](#)]
15. Meng, S.; Kong, T.; Ma, W.; Wang, H.; Zhang, H. 2D crystal-based fibers: Status and challenges. *Small* **2019**, *15*, 1902691. [[CrossRef](#)]
16. Guo, B.; Xiao, Q.; Wang, S.h.; Zhang, H. 2D layered materials: Synthesis, nonlinear optical properties, and device applications. *Laser Photon. Rev.* **2019**, *13*, 1800327. [[CrossRef](#)]
17. Ma, C.; Wang, C.; Gao, B.; Adams, J.; Wu, G.; Zhang, H. Recent progress in ultrafast lasers based on 2D materials as a saturable absorber. *Appl. Phys. Rev.* **2019**, *6*, 041304. [[CrossRef](#)]
18. Shang, C.; Zhang, Y.; Qin, H.; He, B.; Zhang, C.; Sun, J.; Li, J.; Ma, J.; Ji, X.; Xu, L.; et al. Review on wavelength-tunable pulsed fiber lasers based on 2D materials. *Opt. Laser Technol.* **2020**, *131*, 106375. [[CrossRef](#)]
19. Fu, B.; Sun, J.; Wang, G.; Shang, C.; Ma, Y.; Ma, J.; Xu, L.; Scardaci, V. Solution-processed two-dimensional materials for ultrafast fiber lasers. *Nanophotonics* **2020**, *9*, 2169–2189. [[CrossRef](#)]
20. Zhang, A.; Wang, Z.; Ouyang, H.; Lyu, W.; Sun, J.; Cheng, Y.; Fu, B. Recent progress of two-dimensional materials for ultrafast photonics. *Nanomaterials* **2021**, *11*, 1778. [[CrossRef](#)]
21. Zhao, X.; Jin, H.; Liu, J.; Chao, J.; Liu, T.; Zhang, H.; Wang, G.; Lyu, W.; Wageh, S.; Al-Hartomy, O.A.; et al. Integration and applications of nanomaterials for ultrafast photonics. *Laser Photonics Rev.* **2022**, 2200386. [[CrossRef](#)]
22. Set, S.Y.; Yaguchi, H.; Tanaka, Y.; Jablonski, M.; Sakakibara, Y.; Rozhin, A.; Tokumoto, M.; Kataura, H.; Achiba, Y.; Kikuchi, K. Mode-locked fiber lasers based on a saturable absorber incorporating carbon. In Proceedings of the Optical Fiber Communication Conference, Atlanta, GA, USA, 28 March 2003.
23. Bao, Q.; Zhang, H.; Wang, Y.; Ni, Z.; Yan, Y.; Shen, Z.X.; Loh, K.P.; Tang, D.Y. Atomic-layer graphene as a saturable absorber for ultrafast pulsed lasers. *Adv. Funct. Mater.* **2009**, *19*, 3077–3083. [[CrossRef](#)]

24. Hasan, T.; Sun, Z.; Wang, F.; Bonaccorso, F.; Tan, P.H.; Rozhin, A.G.; Ferrari, A.C. Nanotube–polymer composites for ultrafast photonics. *Adv. Mater.* **2009**, *21*, 3874–3899. [[CrossRef](#)]
25. Fu, B.; Hua, Y.; Xiao, X.; Yang, H.; Yang, C.; Sun, Z. Graphene based broadband ultrafast fiber lasers at 1, 1.5 and 2 μm . In Proceedings of the Optics & Photonics Days, Turku, Finland, 20–22 May 2014.
26. Chen, Y.; Jiang, G.; Chen, S.; Guo, Z.; Yu, X.; Zhao, C.; Zhang, H.; Bao, Q.; Wen, S.; Tang, D.; et al. Mechanically exfoliated black phosphorus as a new saturable absorber for both Q-switching and mode-locking laser operation. *Opt. Express* **2015**, *23*, 12823–12833. [[CrossRef](#)] [[PubMed](#)]
27. Li, D.; Jussila, H.; Karvonen, L.; Ye, G.; Lipsanen, H.; Chen, X.; Sun, Z. Polarization and thickness dependent absorption properties of black phosphorus: New saturable absorber for ultrafast pulse generation. *Sci. Rep.* **2015**, *5*, 15899. [[CrossRef](#)]
28. Zhao, C.; Zhang, H.; Qi, X.; Chen, Y.; Wang, Z.; Wen, S.; Tang, D. Ultra-short pulse generation by a topological insulator based saturable absorber. *Appl. Phys. Lett.* **2012**, *101*, 211106. [[CrossRef](#)]
29. Pinghua, T.; Xiaoli, Z.; Chujun, Z.; Yong, W.; Han, Z.; Deyuan, S.; Shuangchun, W.; Dingyuan, T.; Dianyuan, F. Topological insulator: Bi_2Te_3 saturable absorber for the passive Q-switching operation of an in-band pumped 1645-nm Er:YAG ceramic laser. *IEEE Photonics J.* **2013**, *5*, 1500707. [[CrossRef](#)]
30. Zhang, H.; Lu, S.B.; Zheng, J.; Du, J.; Wen, S.C.; Tang, D.Y.; Loh, K.P. Molybdenum disulfide (MoS_2) as a broadband saturable absorber for ultra-fast photonics. *Opt. Express* **2014**, *22*, 7249–7260. [[CrossRef](#)]
31. Xu, B.; Cheng, Y.; Wang, Y.; Huang, Y.; Peng, J.; Luo, Z.; Xu, H.; Cai, Z.; Weng, J.; Moncorge, R. Passively Q-switched Nd:YAlO₃ nanosecond laser using MoS_2 as saturable absorber. *Opt. Express* **2014**, *22*, 28934–28940. [[CrossRef](#)]
32. Jhon, Y.I.; Koo, J.; Anasori, B.; Seo, M.; Lee, J.H.; Gogotsi, Y.; Jhon, Y.M. Metallic MXene saturable absorber for femtosecond mode-locked lasers. *Adv. Mater.* **2017**, *29*, 1702496. [[CrossRef](#)]
33. Fu, B.; Sun, J.; Wang, C.; Shang, C.; Xu, L.; Li, J.; Zhang, H. MXenes: Synthesis, optical properties, and applications in ultrafast photonics. *Small* **2021**, *17*, 2006054. [[CrossRef](#)]
34. Fu, B.; Sun, J.; Cheng, Y.; Ouyang, H.; Compagnini, G.; Yin, P.; Wei, S.; Li, S.; Li, D.; Scardaci, V.; et al. Recent progress on metal-based nanomaterials: Fabrications, optical properties, and applications in ultrafast photonics. *Adv. Funct. Mater.* **2021**, *31*, 2107363. [[CrossRef](#)]
35. Li, X.; An, M.; Li, G.; Han, Y.; Guo, P.; Chen, E.; Hu, J.; Song, Z.; Lu, H.; Lu, J. MOF-derived porous dodecahedron rGO- Co_3O_4 for robust pulse generation. *Adv. Mater. Interfaces* **2022**, *9*, 2101933. [[CrossRef](#)]
36. Li, X.; Xu, W.; Wang, Y.; Zhang, X.; Hui, Z.; Zhang, H.; Wageh, S.; Al-Hartomy, O.A.; Al-Sehemi, A.G. Optical-intensity modulators with PbTe thermoelectric nanopowders for ultrafast photonics. *Appl. Mater. Today* **2022**, *28*, 101546. [[CrossRef](#)]
37. Zhang, C.; Liu, J.; Gao, Y.; Li, X.; Lu, H.; Wang, Y.; Feng, J.-j.; Lu, J.; Ma, K.; Chen, X. Porous nickel oxide micron polyhedral particles for high-performance ultrafast photonics. *Opt. Laser Technol.* **2022**, *146*, 107546. [[CrossRef](#)]
38. Elim, H.I.; Yang, J.; Lee, J.-Y.; Mi, J.; Ji, W. Observation of saturable and reverse-saturable absorption at longitudinal surface plasmon resonance in gold nanorods. *Appl. Phys. Lett.* **2006**, *88*, 083107. [[CrossRef](#)]
39. De Boni, L.; Wood, E.L.; Toro, C.; Hernandez, F.E. Optical saturable absorption in gold nanoparticles. *Plasmonics* **2008**, *3*, 171–176. [[CrossRef](#)]
40. Baida, H.; Mongin, D.; Christofilos, D.; Bachelier, G.; Crut, A.; Maioli, P.; Del Fatti, N.; Vallee, F. Ultrafast nonlinear optical response of a single gold nanorod near its surface plasmon resonance. *Phys. Rev. Lett.* **2011**, *107*, 057402. [[CrossRef](#)]
41. Wang, G.; Liu, T.; Chao, J.; Jin, H.; Liu, J.; Zhang, H.; Lyu, W.; Yin, P.; Al-Ghamdi, A.; Wageh, S.; et al. Recent advances and challenges in ultrafast photonics enabled by metal nanomaterials. *Adv. Opt. Mater.* **2022**, *10*, 2200443. [[CrossRef](#)]
42. Trügler, A. *Optical Properties of Metallic Nanoparticles*; Springer: Berlin/Heidelberg, Germany, 2011.
43. Condorelli, M.; Littl, L.; Pulvirenti, M.; Scardaci, V.; Meneghetti, M.; Compagnini, G. Silver nanoplates paved PMMA cuvettes as a cheap and re-usable plasmonic sensing device. *Appl. Surf. Sci.* **2021**, *566*, 150701. [[CrossRef](#)]
44. Jiang, T.; Xu, Y.; Tian, Q.; Liu, L.; Kang, Z.; Yang, R.; Qin, G.; Qin, W. Passively Q-switching induced by gold nanocrystals. *Appl. Phys. Lett.* **2012**, *101*, 151122. [[CrossRef](#)]
45. Kang, Z.; Li, Q.; Gao, X.J.; Zhang, L.; Jia, Z.X.; Feng, Y.; Qin, G.S.; Qin, W.P. Gold nanorod saturable absorber for passive mode-locking at 1 μm wavelength. *Laser Phys. Lett.* **2014**, *11*, 035102. [[CrossRef](#)]
46. Kang, Z.; Liu, M.Y.; Gao, X.J.; Li, N.; Yin, S.Y.; Qin, G.S.; Qin, W.P. Mode-locked thulium-doped fiber laser at 1982 nm by using a gold nanorods saturable absorber. *Laser Phys. Lett.* **2015**, *12*, 045105. [[CrossRef](#)]
47. Naharuddin, N.Z.A.; Abu Bakar, M.H.; Sadrolhosseini, A.R.; Tamchek, N.; Alresheedi, M.T.; Abas, A.F.; Mahdi, M.A. Pulsed-laser-ablated gold-nanoparticles saturable absorber for mode-locked erbium-doped fiber lasers. *Opt. Laser Technol.* **2022**, *150*, 107875. [[CrossRef](#)]
48. Zheng, C.; Wenzhe, C.; Xiaoyun, Y.; Cai, S.; Xiao, X. Fabricating silver nanoplate/hybrid silica gel glasses and investigating their nonlinear optical absorption behavior. *Opt. Mater.* **2014**, *36*, 982–987. [[CrossRef](#)]
49. Condorelli, M.; Scardaci, V.; Pulvirenti, M.; D’Urso, L.; Neri, F.; Compagnini, G.; Fazio, E. Surface plasmon resonance dependent third-order optical nonlinearities of silver nanoplates. *Photonics* **2021**, *8*, 299. [[CrossRef](#)]
50. Konda, S.R.; Maurya, S.K.; Ganeev, R.A.; Lai, Y.H.; Guo, C.; Li, W. Third-order nonlinear optical effects of silver nanoparticles and third harmonic generation from their plasma plumes. *Optik* **2021**, *245*, 167680. [[CrossRef](#)]

51. Mohamed, T.; El-Motlak, M.H.; Mamdouh, S.; Ashour, M.; Ahmed, H.; Qayyum, H.; Mahmoud, A. Excitation wavelength and colloids concentration-dependent nonlinear optical properties of silver nanoparticles synthesized by laser ablation. *Materials* **2022**, *15*, 7348. [[CrossRef](#)]
52. Ahmad, H.; Samion, M.Z.; Muhamad, A.; Sharbirin, A.S.; Ismail, M.F. Passively Q-switched thulium-doped fiber laser with silver-nanoparticle film as the saturable absorber for operation at 2.0 μm . *Laser Phys. Lett.* **2016**, *13*, 126201. [[CrossRef](#)]
53. Rosdin, R.Z.R.R.; Ahmad, M.T.; Muhammad, A.R.; Jusoh, Z.; Arof, H.; Harun, S.W. Nanosecond pulse generation with silver nanoparticle saturable absorber. *Chin. Phys. Lett.* **2019**, *36*, 054202. [[CrossRef](#)]
54. Fu, B.; Wang, P.; Li, Y.; Condorelli, M.; Fazio, E.; Sun, J.; Xu, L.; Scardaci, V.; Compagnini, G. Passively Q-switched Yb-doped all-fiber laser based on Ag nanoplates as saturable absorber. *Nanophotonics* **2020**, *9*, 3873–3880. [[CrossRef](#)]
55. Fu, B.; Zhang, C.; Wang, P.; Condorelli, M.; Pulvirenti, M.; Fazio, E.; Shang, C.; Li, J.; Li, Y.; Compagnini, G.; et al. Nonlinear optical properties of Ag nanoplates plasmon resonance and applications in ultrafast photonics. *J. Light. Technol.* **2021**, *39*, 2084–2090. [[CrossRef](#)]
56. Fathima, R.; Mujeeb, A. Nonlinear optical investigations of laser generated gold, silver and gold-silver alloy nanoparticles and optical limiting applications. *J. Alloy. Compd.* **2021**, *858*, 157667. [[CrossRef](#)]
57. Sackuvich, R.K.; Peppers, J.M.; Myoung, N.; Badikov, V.V.; Fedorov, V.V.; Mirov, S.B. Spectroscopic characterization of $\text{Ti}^{3+}:\text{AgGaS}_2$ and $\text{Fe}^{2+}:\text{MgAl}_2\text{O}_4$ crystals for mid-IR laser applications. In Proceedings of the Solid State Lasers XXI: Technology and Devices, San Francisco, CA, USA, 22–25 January 2012; pp. 427–432.
58. Cesca, T.; García-Ramírez, E.V.; Sánchez-Esquivel, H.; Michieli, N.; Kalinic, B.; Gómez-Cervantes, J.M.; Rangel-Rojo, R.; Reyes-Esqueda, J.A.; Mattei, G. Dichroic nonlinear absorption response of silver nanoprism arrays. *RSC Adv.* **2017**, *7*, 17741–17747. [[CrossRef](#)]
59. Compagnini, G.; Condorelli, M.; Fragalà, M.E.; Scardaci, V.; Tinnirello, I.; Puglisi, O.; Neri, F.; Fazio, E. Growth kinetics and sensing features of colloidal silver nanoplates. *J. Nanomater.* **2019**, *2019*, 7084731. [[CrossRef](#)]
60. Scardaci, V. Anisotropic silver nanomaterials by photochemical reactions: Synthesis and applications. *Nanomaterials* **2021**, *11*, 2226. [[CrossRef](#)] [[PubMed](#)]
61. Bai, X.; Mou, C.; Xu, L.; Wang, S.; Pu, S.; Zeng, X. Passively Q-switched erbium-doped fiber laser using Fe_3O_4 -nanoparticle saturable absorber. *Appl. Phys. Express* **2016**, *9*, 042701. [[CrossRef](#)]
62. Ahmad, H.; Reduan, S.A.; Yusoff, N. Chitosan capped nickel oxide nanoparticles as a saturable absorber in a tunable passively Q-switched erbium doped fiber laser. *RSC Adv.* **2018**, *8*, 25592–25601. [[CrossRef](#)]
63. Ahmad, H.; Lee, C.S.; Ismail, M.A.; Ali, Z.A.; Reduan, S.A.; Ruslan, N.E.; Harun, S.W. Tunable Q-switched fiber laser using zinc oxide nanoparticles as a saturable absorber. *Appl. Opt.* **2016**, *55*, 4277–4281. [[CrossRef](#)]
64. Guo, J.; Zhang, H.; Zhang, C.; Li, Z.; Sheng, Y.; Li, C.; Bao, X.; Man, B.; Jiao, Y.; Jiang, S. Indium tin oxide nanocrystals as saturable absorbers for passively Q-switched erbium-doped fiber laser. *Opt. Mater. Express* **2017**, *7*, 3494–3502. [[CrossRef](#)]
65. Hisamuddin, N.; Jusoh, Z.; Zakaria, U.N.; Zulkifli, M.Z.; Latiff, A.A.; Yasin, M.; Ahmad, H.; Harun, S.W. Q-switched Raman fiber laser with titanium dioxide based saturable absorber. *Optoelectron. Adv. Mater.* **2017**, *11*, 127–130.
66. Wang, X.-D.; Liang, Q.-M.; Luo, A.-P.; Luo, Z.-C.; Liu, M.; Zhu, Y.-F. Mode locking and multiwavelength Q-switching in a dumbbell-shaped fiber laser with a gold nanorod saturable absorber. *Opt. Eng.* **2019**, *58*, 056113. [[CrossRef](#)]
67. Muhammad, A.R.; Ahmad, M.T.; Zakaria, R.; Rahim, H.R.A.; Yusoff, S.F.A.Z.; Hamdan, K.S.; Yusof, H.H.M.; Arof, H.; Harun, S.W. Q-switching pulse operation in 1.5- μm region using copper nanoparticles as saturable absorber. *Chin. Phys. Lett.* **2017**, *34*, 034205. [[CrossRef](#)]